Supplemental Materials

Molecular Biology of the Cell

Mills et al.

Mills, Brocardo and Henderson: Supplementary Information

Supplementary Materials and Methods

Computational mitochondrial distribution analysis

For key experimental results, a more rigorous computational analysis of mitochondrial distribution was performed on a randomly selected subset of cells (n=30) for each sample. Images of fixed cells stained for APC and mitochondria were collected as described previously, and analysis by ImageJ was used to determine the zonal distribution (Figure 1B) of mitochondria in each cell. To do this, the nucleus and the cell membrane, identified by DIC image capture, were marked and the mitochondrial fluorescent staining was thresholded to generate binary images. Straight lines were drawn radiating from the nucleus to the cell membrane, measured into thirds and connected to adjacent lines dividing the cell into the three zones which formed concentric shapes around the nucleus. The 'analyze particles' function was used to determine the total volume of mitochondria in the cell and each zone, before defined parameters were used to classify each cell into a particular Zone according to the percentage of total cellular mitochondria present (see Figure S2B).

Cell culture and treatments

Stable HEK293 cell lines inducible for APC-WT and APC-1309 (kindly provided by and described in (Tighe *et al.*, 2004)) were cultured in DMEM containing 15 g/ml blasticidin and 150 g/ml hygromycin B under standard conditions. APC protein expression was induced by the addition of 2 ng/ml tetracycline 16 h prior to subsequent processing. Wnt3a conditioned media kindly provided by Dr Linda Bendall (The Westmead Institute).

Tighe, A., Johnson, V.L., and Taylor, S.S. (2004). Truncating APC mutations have dominant effects on proliferation, spindle checkpoint control, survival and chromosome stability. J Cell Sci *117*, 6339-6353.

Figure Legends

Figure S1: Specificity of APC influence on mitochondria distribution. (A,B) Loss of wild type APC induces a redistribution of mitochondria to the perinuclear region in HDF1314 and NIH 3T3 cells stained with CMX-Ros. APC was silenced in HDF1314 and NIH 3T3 cells using pooled APC#1/APC#2 siRNA or mAPC1 siRNA, respectively. Cells were analyzed by DeltaVision immunofluorescence microscopy after staining for mitochondria (CMX-Ros) and APC. (A) Representative images are shown (HDF1314 not shown). (B) Cells were scored for mitochondrial distribution, revealing a redistribution of mitochondria from membrane towards the perinuclear region (zone 1) with APC siRNAs. (C) To confirm the effect of APC using a different mitochondria marker, APC was silenced in U2OS cells and counterstained with antibodies against mitochondrial HSP70 and APC. Loss of APC also induced a significant (***, $P<0.001$) redistribution of mitochondria. Bar graph data presented as mean (±S.D.), statistical analysis by unpaired two tailed T-test. (D-I) Control experiments reveal the specific influence of APC on mitochondrial distribution patterns. Cells were

treated 1 h with DMSO or the microtubule depolymerising agent, nocodazole (33μM, Sigma), and analysed by (D) immunofluorescence microscopy after staining for mitochondria (CMX-Ros) and microtubules (α-tubulin). Cell scoring (F) revealed a significant (**, $P<0.01$) shift of mitochondria towards the perinuclear region following destruction of the microtubule network. (E) Cells were treated 1 h with DMSO or the actin depolymerising agent, latrunculin A (0.5nM, Sigma), and analysed by immunofluorescence microscopy after staining for mitochondria (CMX-Ros) and actin filaments (actin). (F) Cell scoring revealed no changes (n.s., not significant) in mitochondrial localisation following destruction of the actin network, at latrunculin A concentrations that left the microtubule network intact. (G) Cells were treated with control or APC#1 siRNA and 48 h later analyzed by immunofluorescence microscopy after staining for different organelles: the endoplastic reticulum (ER-Tracker), golgi (58k; Abcam Ab), lysosomes (LAMP-1; Becton Dickinson Ab) or centrosomes (γ-tubulin; Abcam Ab). Representative cell images are shown. (H) Loss of APC was confirmed by western blot analysis. Topoisomerase II was used as a loading control. (I) Cell organelles were scored for distribution into 'zones'. No significant alterations in distribution patterns were observed following loss of APC. Significant differences for perinuclear distribution relative to controls are indicated (n.s., not significant). Scale bars denote 10 μm.

Figure S2: Quantitative analysis of mitochondrial distribution using ImageJ. (A) Cells were analyzed for mitochondrial distribution and classified into different 'zones' (spanning 33%, 66% and 100% of the distance between the nucleus and plasma membrane, upper left) which were defined according to the proportion of mitochondria present in each zone (upper right). Fluorescent images of fixed cells stained for mitochondria were acquired using the DeltaVision microscope and subjected to deconvolution. Mitochondrial fluorescent staining was thresholded using ImageJ to create a binary image which was then measured and segmented into zones for determination of mitochondrial volume (lower). (B) Representative examples are shown of cells from each cell line analyzed by ImageJ computational analysis (upper) and data readouts for each example (lower). (C) Images of U2OS, SW480, HT-29, HCT116 and LIM1215 cells treated with control or APC siRNAs and stained for mitochondria were subjected to ImageJ analysis of mitochondria in the different zones. The distribution patterns mirrored those previously observed by visual scoring (Fig. 2B). We note that the APC knockdown clearly shifted mitochondria toward the nucleus in LIM1215 cells, although the pattern of change in these cells was not quite as strong as observed by visual scoring (Fig. 2B). (D) Images of HT-29 cells expressing GFP or GFP-APC-WT, stained for mitochondria were analyzed by ImageJ to determine mitochondrial zonal distribution. Results mirrored those previously observed when scored by eye.

Figure S3: Wild-type APC interacts with Miro-1 and Milton-2 at mitochondria. (A) Lysates from HEK293 cell lines with induced expression of APC-1309 (left panel) or APC-wild type (right panel) were immunoprecipitated with antibodies against APC. Analysis by western blot revealed that the APC antibody could capture Miro in cells induced for APC-wild type, but not APC-1309. (B) Hela cells were subject to Duolink PLA to visualize interactions between APC/Miro-1 and APC/Milton-2 *in situ* using antibodies against APC, Miro-1 and Milton-2. Representative images (B) and scoring (C) from analysis by immunofluorescence microscopy indicate a positive PLA signal (green dot) between APC/Miro-1 and APC/Milton-2, which is absent when each antibody is tested alone. (D) Duolink PLA was employed in U2OS cells to

visualize APC/Milton interactions *in situ* using antibodies against APC and Milton-2. Mitochondrial counterstaining (CMX-Ros) and immunofluorescence microscopy revealed APC/Milton-2 PLA signals (green dots) localized to the mitochondria as shown in the 3D image projection. (E-F) Mitochondrial counterstaining (CMX-Ros) in Hela cells and scoring of immunofluorescence images show that APC/Miro-1 and APC/Milton-2 PLA signals localize to the mitochondria (E), as demonstrated in the 3D image projections (F). Box and whisker plots represent the median (line), upper/lower quartile (box) and min/max (error bars with 95% C.I). Bar graph data presented as mean (±S.D.). Scale bars denote 10 μm.

Figure S4: GFP APC(2650-2843) interacts with Miro-1 and Milton-2 by Duolink PLA. (A,B) GFP-APC fragments and Miro-1 were analyzed for their ability to form protein complexes *in situ* by Duolink PLA using antibodies against GFP and Miro-1. Scoring of PLA signals per cell as indicated in the box and whisker plot (A) and table (B), revealed that only one fragment, GFP APC (2650-2843), displayed a signal above the GFP background (~3.4 fold, ***P<0.001), indicative of a positive interaction. Statistical significance of PLA signal per cell for other fragments relative to mean was not significant (n.s.). *Fold change relative to GFP control; n, number in sample; IQR, inter-quartile range. (C) Association of GFP-APC(2650-2843) with endogenous Miro was confirmed by immunoprecipitation of Miro by anti-GFP using lysate from transfected U2OS cells. The Miro-1 IP band detected migrated at a slightly larger size than the major band, suggesting a possible post-translationally modified form of Miro-1 (see Discussion). This band was not observed in transfected U2OS cells expressing GFP, GFP-APC(1-302) or GFP-APC(1379-2080). (D-F) U2OS cells expressing GFP or GFP APC (2650-2843) were analyzed for their ability to form protein complexes *in situ* with Milton-2 by Duolink PLA using antibodies against GFP and Milton-2. (D) Representative cell images from analysis by immunofluorescent microscopy are shown, with PLA GFP/Milton-2 complexes indicated by red dots. Scoring of PLA signals per cell, as indicated in the box and whisker plot (E) and table (F), revealed that GFP APC (2650-2843) displayed a positive signal above the GFP background (~2.6 fold, *** P<0.001). *Fold change relative to GFP control; n, number in sample; IQR, inter-quartile range. Box and whisker plot represent the median (line), upper/lower quartile (box) and min/max (error bars with 95% C.I), statistical analysis by unpaired one tailed T-test. Scale bars denote 10 μm.

Figure S5: Truncation or loss of APC is not required for the interaction between Milton-2 and KIF5 or for mitochondrial localization of Miro-1 and stimulation of the canonical Wnt pathway does not affect mitochondrial distribution. (A,B) Duolink PLA was utilized to detect interactions between KIF5 and Milton-2 in U2OS (full length APC) and SW480 (APC 1337) cell lines, which were subject to analysis by immunofluorescence microscopy. (A) Representative images are shown and scoring, as indicated in the box and whisker plot (B), showed a positive interaction for Milton-2/KIF5 in both U2OS and SW480. (C,D) U2OS cells were treated with control or APC #1 siRNA and counterstained for mitochondria (CMX-Ros) and Miro-1 and (C) analyzed by immunofluorescence microscopy. (D) Colocalization analysis showed no changes in mitochondrial localization of Miro-1 following loss of APC. Scale bars denote 10 μm. (E) U2OS cells were treated with control or APC #1 siRNA prior to exposure to control L-cell conditioned media (LCM) or Wnt3a conditioned media (Wnt) for 6h. Mitochondrial distribution in fixed cells was analyzed by immunofluorescence microscopy after staining for mitochondria (CMX-Ros). Bar graph data presented as mean (±S.D).

Supplementary Videos 1 & 2

Mitochondrial movement in migrating cells transfected with GFP2-Mito and either (1) control or (2) mAPC-red siRNAs. Images were acquired every 7 seconds for a total of 5 mins. The middle planes of z-stacks were acquired from time-lapse live cell imaging, and analysed using MTrackJ, then compressed into AVI files using ImageJ at a rate of 5 frames per second.

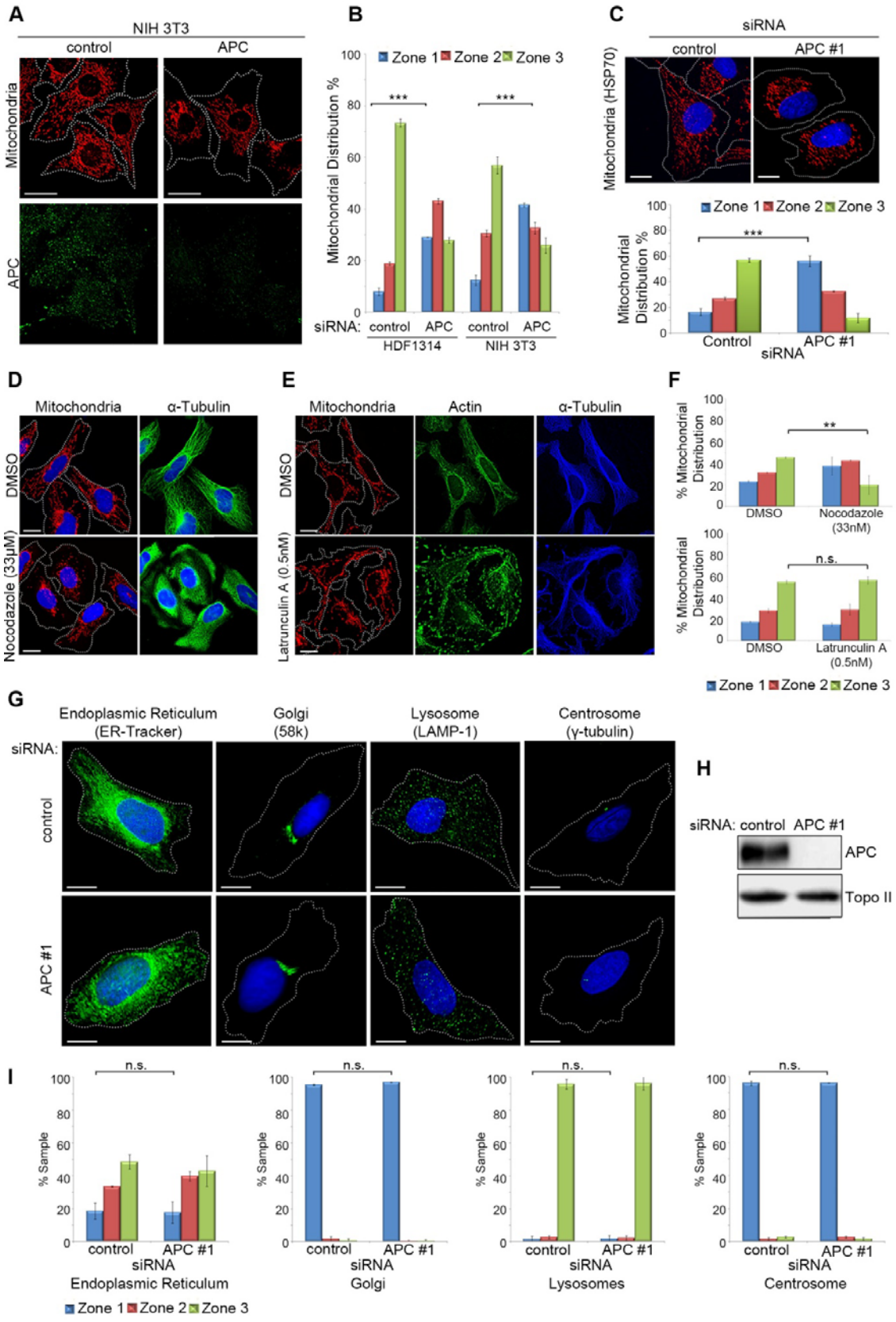
A
NIH 3T3
control
APC
Mitochondria
APC
B
Zone 1 Zone 2 Zone 3
Mitochondrial Distribution %
***
***
siRNA: control APC control APC
HDF1314
NIH 3T3
C
siRNA
control
APC #1
Mitochondria (HSP70)
Zone 1 Zone 2 Zone 3
Mitochondrial Distribution %
***
Control
APC #1
siRNA
D
Mitochondria
α-Tubulin
DMSO
Nocodazole (33μM)
E
Mitochondria
Actin
α-Tubulin
DMSO
Latrunculin A (0.5nM)
F
% Mitochondrial Distribution
**
DMSO
Nocodazole (33nM)
% Mitochondrial Distribution
n.s.
DMSO
Latrunculin A (0.5nM)
Zone 1 Zone 2 Zone 3
G
siRNA:
Endoplasmic Reticulum (ER-Tracker)
Golgi (58k)
Lysosome (LAMP-1)
Centrosome (γ-tubulin)
control
APC #1
H
siRNA: control APC #1
APC
Topo II
I
n.s.
% Sample
control
APC #1
siRNA
Endoplasmic Reticulum
Golgi
Lysosomes
Centrosome
Zone 1 Zone 2 Zone 3

Fig. S1

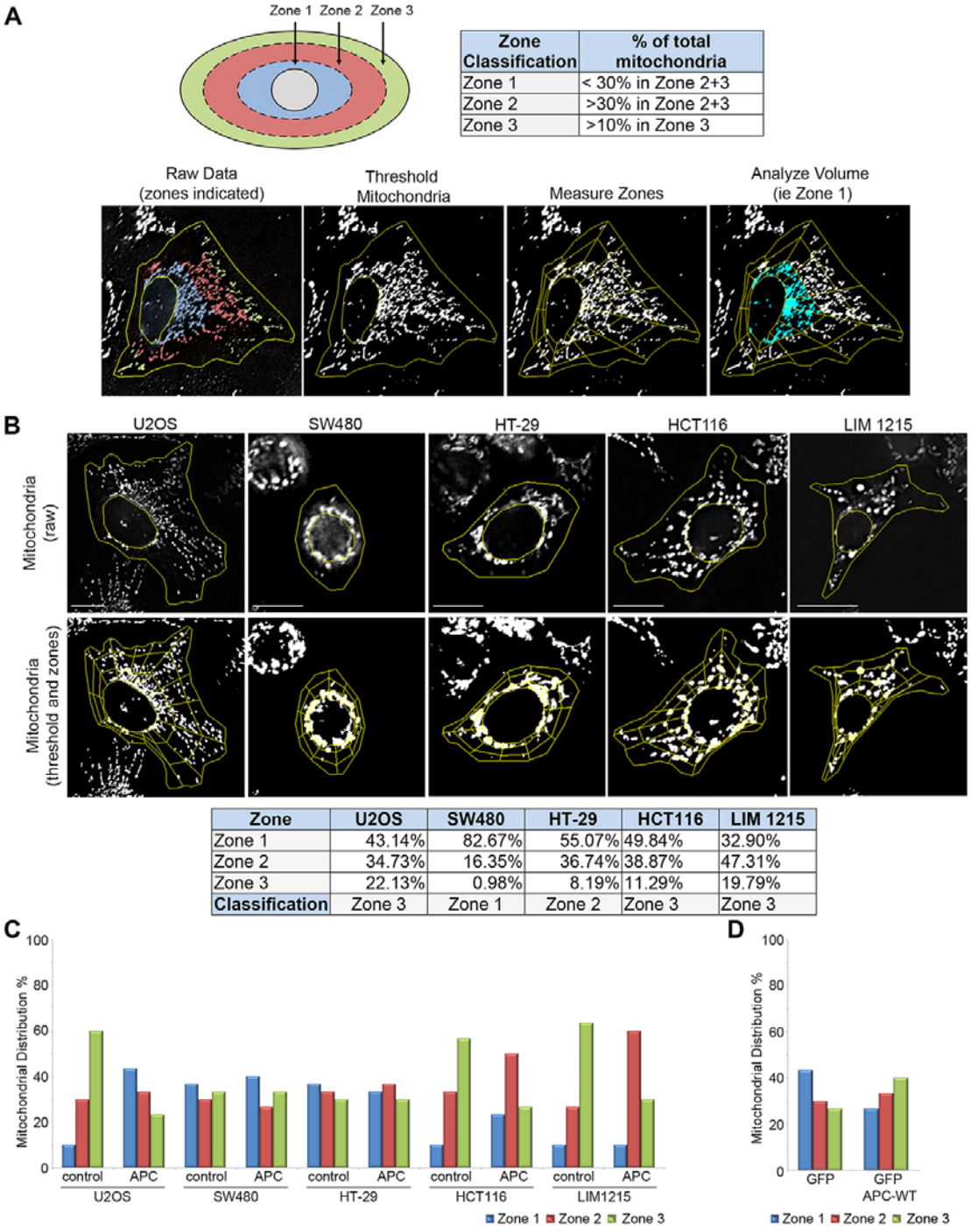

Zone Classification	% of total mitochondria
Zone 1	< 30% in Zone 2+3
Zone 2	>30% in Zone 2+3
Zone 3	>10% in Zone 3

Zone	U2OS	SW480	HT-29	HCT116	LIM 1215
Zone 1	43.14%	82.67%	55.07%	49.84%	32.90%
Zone 2	34.73%	16.35%	36.74%	38.87%	47.31%
Zone 3	22.13%	0.98%	8.19%	11.29%	19.79%
Classification	Zone 3	Zone 1	Zone 2	Zone 3	Zone 3

Fig. S2

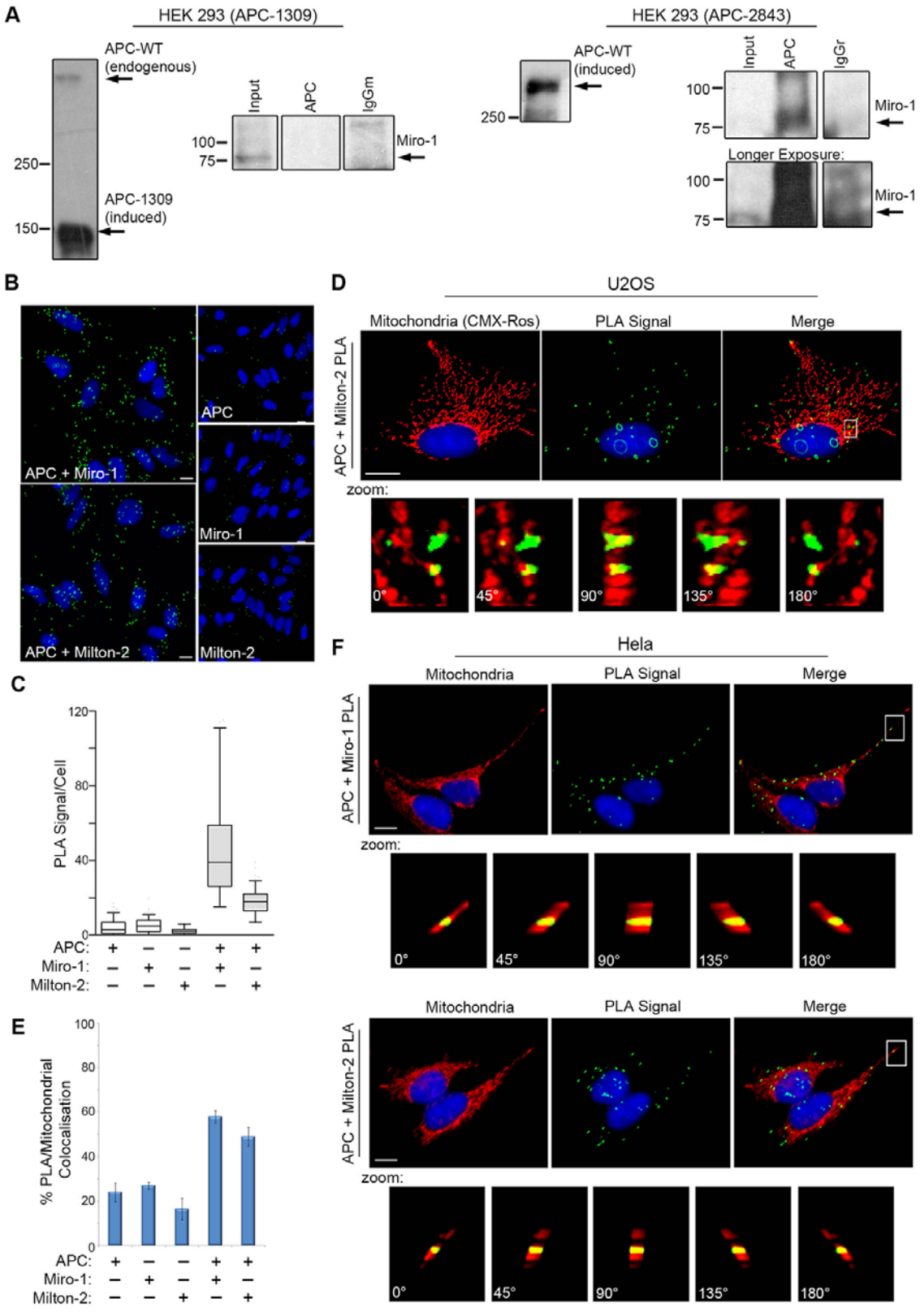
A
HEK 293 (APC-1309)
APC-WT
(endogenous)
APC-1309
(induced)
250
150
Input
APC
IgGm
100
75
Miro-1
HEK 293 (APC-2843)
APC-WT
(induced)
250
Input
APC
IgGr
100
75
Miro-1
Longer Exposure:
100
75
Miro-1
B
APC + Miro-1
APC
Miro-1
APC + Milton-2
Milton-2
C
PLA Signal/Cell
120
80
40
0
APC:
Miro-1:
Milton-2:
D
U2OS
Mitochondria (CMX-Ros)
PLA Signal
Merge
APC + Milton-2 PLA
zoom:
0°
45°
90°
135°
180°
E
% PLA/Mitochondrial Colocalisation
100
80
60
40
20
0
APC:
Miro-1:
Milton-2:
F
Hela
Mitochondria
PLA Signal
Merge
APC + Miro-1 PLA
zoom:
0°
45°
90°
135°
180°
Mitochondria
PLA Signal
Merge
APC + Milton-2 PLA
zoom:
0°
45°
90°
135°
180°

Fig. S3

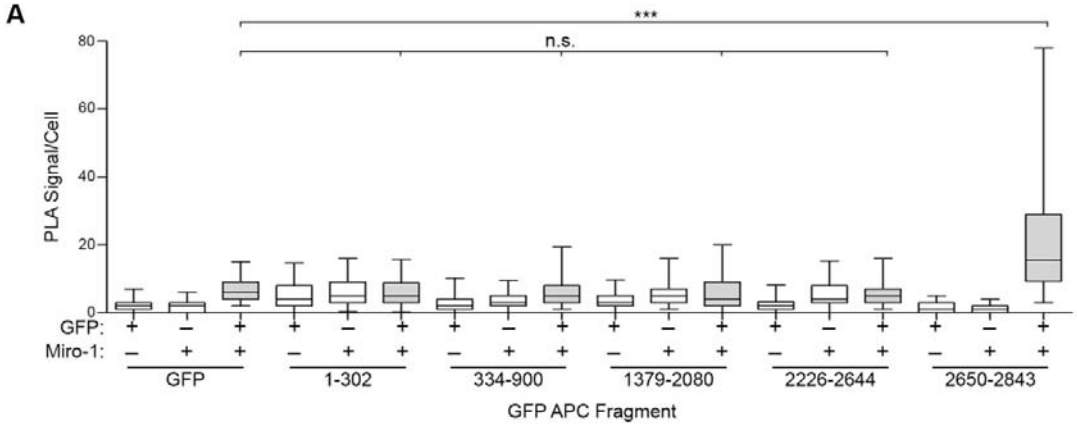

B

Fragment	Antibody	n	Mean	Fold Change*	Median	IQR	Min	Max	SD
GFP	GFP	161	2.4		2.0	2.0	0	10	2.25
	Miro	156	2.1		2.0	3.0	0	12	2.10
	GFP + Miro	184	7.1	1.0	6.0	5.0	1	25	4.37
(1-302)	GFP	126	5.3		4.0	6.0	0	22	4.40
	Miro	107	6.2		5.0	6.0	0	26	4.97
	GFP + Miro	124	6.1	0.9	5.0	5.8	0	19	4.55
(334-900)	GFP	134	3.2		2.0	3.0	0	24	3.45
	Miro	128	3.9		3.0	3.0	0	14	2.74
	GFP + Miro	130	6.6	0.9	5.0	5.0	0	29	5.66
(1379-2080)	GFP	112	3.8		3.0	3.0	0	19	3.28
	Miro	107	6.0		5.0	4.0	0	32	5.48
	GFP + Miro	97	6.4	0.9	4.0	7.0	0	31	6.40
(2226-2644)	GFP	118	2.9		2.0	2.3	0	24	3.89
	Miro	117	5.9		4.0	5.0	0	31	5.15
	GFP + Miro	128	6.0	0.8	5.0	4.0	0	32	4.91
(2650-2843)	GFP	140	1.9		1.0	3.0	0	12	2.20
	Miro	152	1.3		1.0	2.0	0	6	1.37
	GFP + Miro	148	23.9	3.4	15.5	19.8	0	100	22.66

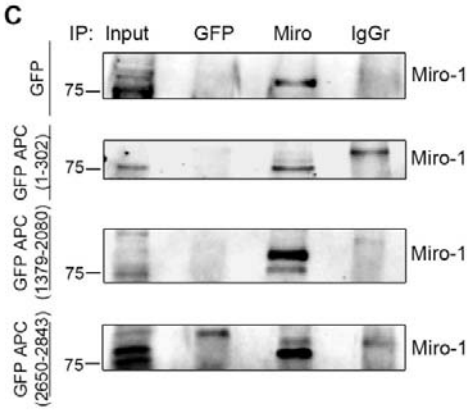

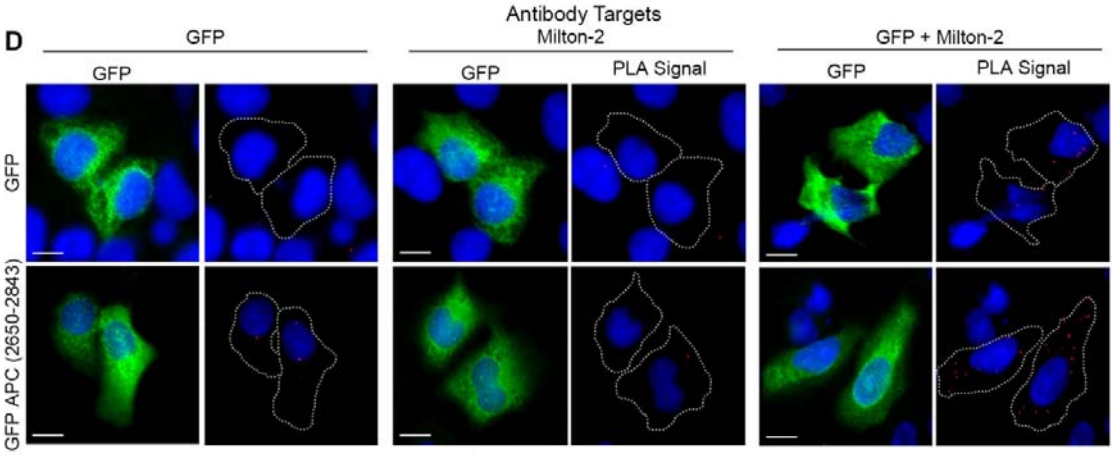

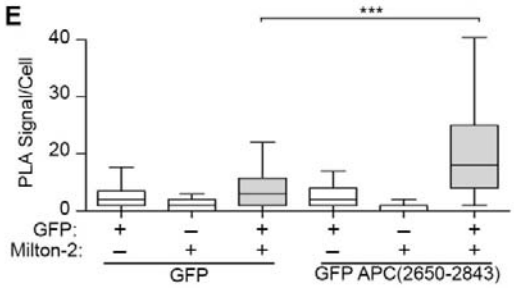

F

GFP	Antibody	n	Mean	Fold Change*	Median	IQR	Min	Max	SD
GFP	GFP	105	2.58		2	2.5	0	12	2.47
	Milton-2	106	1.05		1	2	0	6	1.24
	GFP + Milton-2	108	3.93	1.00	3	4.75	0	16	3.50
APC (2650-2843)	GFP	115	2.50		2	3	0	8	2.03
	Miro-1	101	0.72		0	1	0	4	0.88
	GFP + Milton-2	92	10.29	2.6	8	11	0	40	8.94

Fig. S4

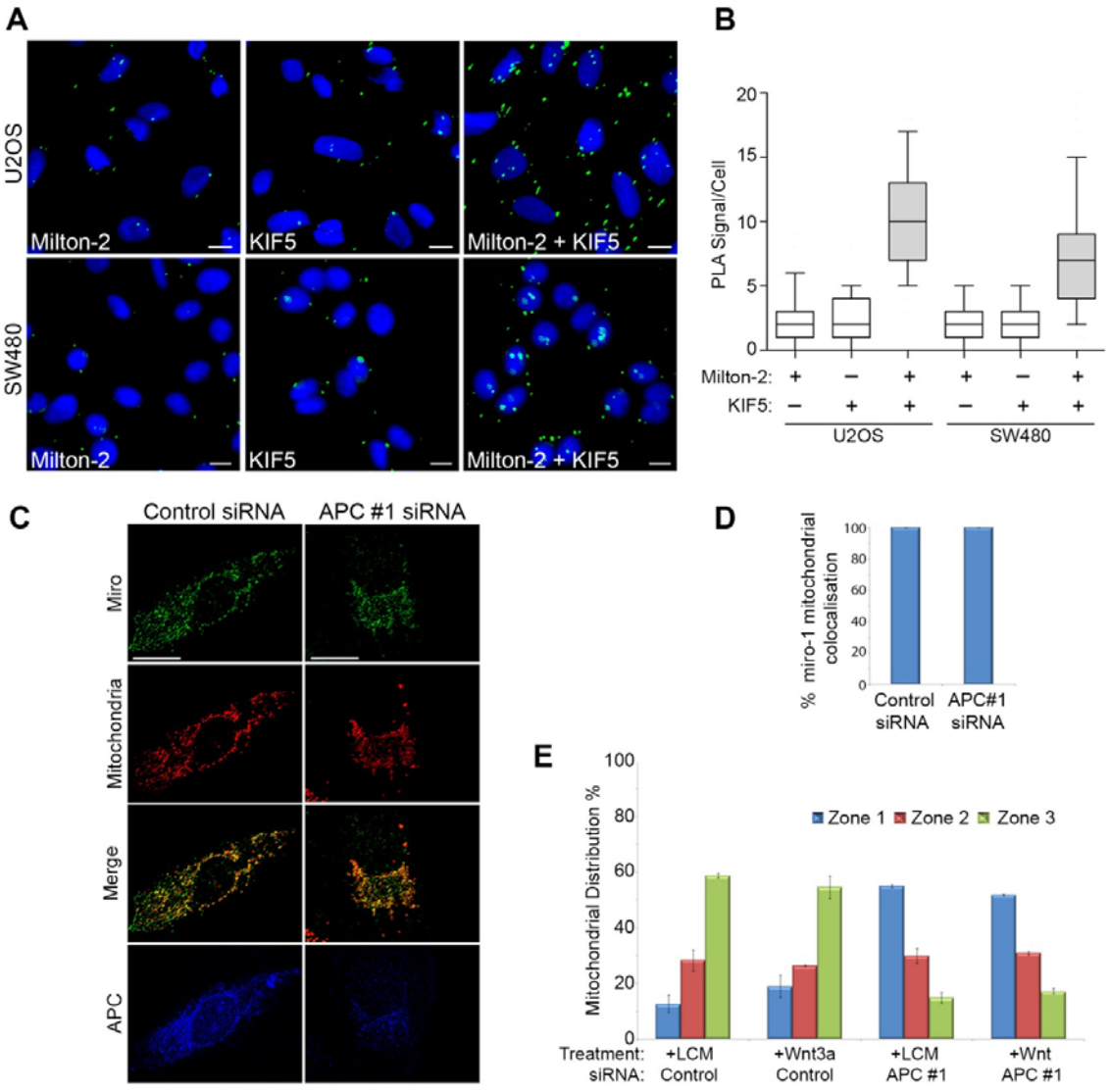
A
U2OS
SW480
Milton-2
KIF5
Milton-2 + KIF5
B
PLA Signal/Cell
20
15
10
5
0
Milton-2:
KIF5:
U2OS
SW480
C
Control siRNA
APC #1 siRNA
Miro
Mitochondria
Merge
APC
D
% miro-1 mitochondrial colocalisation
100
80
60
40
20
0
Control siRNA
APC#1 siRNA
E
Mitochondrial Distribution %
Zone 1
Zone 2
Zone 3
Treatment:
siRNA:
+LCM Control
+Wnt3a Control
+LCM APC #1
+Wnt APC #1

Fig. S5